Monatshefte für Chemie - Chemical Monthly (2020) 151:1557–1567
https://doi.org/10.1007/s00706-020-02687-2

ORIGINAL PAPER

The (NHC)$PdBr_2$(2-aminopyridine) complexes: synthesis, characterization, molecular docking study, and inhibitor effects on the human serum carbonic anhydrase and serum bovine xanthine oxidase

Ferhat Türker[1] · Samir Abbas Ali Noma[1] · Aydın Aktaş[1,2] · Khattab Al-Khafaji[3] · Tugba Taşkın Tok[3,4] · Burhan Ateş[1] · Yetkin Gök[1]

Received: 30 December 2019 / Accepted: 14 September 2020 / Published online: 16 October 2020

Abstract

This study contains the synthesis, spectral analysis, and the enzyme inhibition effects of the Pd-based complexes bearing both 2-aminopyridine and *N*-heterocyclic carbene (NHC) ligands. The NHC ligand in the Pd-based complexes contains the 3-cyanobenzyl group. All new complexes were synthesized from (NHC)$PdBr_2$(pyridine) complexes and 2-aminopyridine. These new complexes were characterized by using elemental analysis, ^{1}H NMR, ^{13}C NMR, and FT-IR spectroscopy techniques. Furthermore, inhibitor effects of these complexes were also tested toward some metabolic enzymes such as carbonic anhydrase and xanthine oxidase enzymes. The IC_{50} range for hCA I, hCA II, and XO were determined as 0.325–0.707, 0.238–0.636, and 0.576–1.693 µM, respectively. These data showed that Pd(II)–NHC complexes bearing 2-aminopyridine may be potent inhibitors of hCA and XO enzymes. Besides these applications, molecular docking was performed by using CDOCKER tool as a part of Discovery studio 2019, not only to determine the binding mode of synthesized inhibitors, but also to determine the correlation between the CDOCKER score values and IC_{50} values. We found a good correlation ($R^2 = 0.7403$) between IC_{50} and the CDOCKER score of the inhibitors for XO. These findings could be a reference to start the development of effective medicine for XO.

Graphic abstract

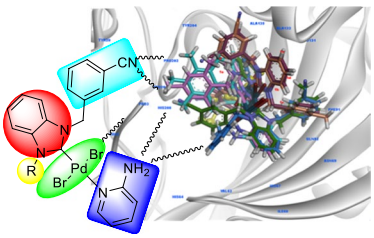

Keywords 2-Aminopyridine · Carbonic anhydrase · Enzyme inhibition · *N*-heterocyclic carbene · Molecular docking · Palladium complexes · Xanthine oxidase

Introduction

Since half a century ago, the NHCs have attracted a great deal of interest as ligands in the fields of organic and organometallic chemistry after the discovery of the stable metal–NHC complexes by Wanzlick [1]. Surprisingly, NHCs have been overshadowed by metal-NHC complexes

Electronic supplementary material The online version of this article (https://doi.org/10.1007/s00706-020-02687-2) contains supplementary material, which is available to authorized users.

✉ Aydın Aktaş
aydinaktash@hotmail.com

Extended author information available on the last page of the article

for 23 years. In the early 1990s, stable, isolated and storable crystal NHC 1,3-di(adamantyl)imidazol-2-ylidene (IAd) was reported by Arduengo et al. [2, 3].

The NHCs have important properties such as high reactivity, structural diversity, being a strong σ-donor and a weak π-acceptor. Furthermore, the stability of the metal–carbene bond in the metal–NHC complexes increased the interest in these complexes [4–9]. The NHCs can form stable complexes with almost all transition metals. Stable metal–NHC complexes of many transition metals such as Pt [10], Ru [11, 12], Pd [13], Fe [14], Ni [15], Co [16], Zn [17], Mn [18], Hg [19], Ag [20], Cu [21], and Au [22] have already been synthesized. In the beginning, the synthesized metal–NHC complexes were used as active catalysts in various catalytic reactions [23–27]. Subsequently, biochemists have become interested in the biological properties of these complexes [28, 29]. In particular, studies on the medical applications of the metal–NHC complexes containing the Au [30], Ru [31], Pt [32], and Ag [33] transition metals have increased. Recently, studies on the medical applications of Pd(II)NHC complexes have been published [28, 29, 34–36]. However, there is only one recent study concerning the medical applications of Pd-based complexes containing both 2-aminopyridine and NHC ligands [29].

Carbonic anhydrase (CA) is a zinc metalloenzyme that plays an important role in biological systems [37]. CAs are also vital in maintaining physiological and pathophysiological processes. Therefore, the inhibition of CAs is a useful way for healing some disease such as cancer [38], and obesity cases [39]. CA catalyzes the conversion to HCO_3^- by giving the proton of H_2O to CO_2. Thus, it keeps up the acid–base balance in the blood and other tissues and helps to move out CO_2 from biological systems [40], ion exchange, and cardiovascular system organization [41]. Whereas the inhibitors-oriented hCA I are beneficial in retinal and cerebral edema, inhibitors-oriented hCA II are utilized as diuretics, in edema management, as antiglaucoma substances, anti-epilepsy drugs, and additionally for altitude sickness therapy [42].

Xanthine oxidase (XO, EC 1.17.3.2) is a flavor-protein enzyme and has high activity in the liver and intestine. XO is highly concentrated in the gastrointestinal tract [43]. XO is an enzyme that has major activities such as the hydroxylation of hypoxanthine to xanthine and xanthine to uric acid [44]. During the reaction process, an increase in reactive oxygen species (ROS) level is considered [45]. Therefore, XO is an important source of ROS and uric acid. Excessive manufacture of uric acid may cause hyperuricemia, which is the key for gout disease [46]. The increment of XO level can give rise to oxidative stress, mutagenesis, and perhaps cause cancer. Because of these, inhibition of XO decreases oxidative stress immediately after inflammation. Furthermore, the inhibition of XO may be a way for cancer cure [47].

We had previously synthesized Pd-based complexes bearing the PPh_3/NHC [8, 27, 48], and the morpholine/NHC ligand mixture [28]. In this study, we have synthesized new Pd-based complexes bearing NHC/2-aminopyridine ligand mixture from Pd-PEPPSI (pyridine-enhanced precatalyst preparation stabilization and initiation) complexes and 2-aminopyridine. These new complexes contain two important functional groups, such as benzonitrile ($–C_6H_5CN$) and aminopyridine ($–C_5H_4NNH_2$). The benzonitrile core present in many chemical structures such as natural products, pharmaceuticals, and agrochemicals makes such molecules interesting targets among many chemicals [49, 50]. Moreover, the nitrile group in benzonitriles represents one of the most commonly used functional groups and can be applied to other functional groups such as aldehydes, carboxylic acids, amidines, amides, and amines [51]. The complexes containing electrophilic groups such as benzonitriles, commonly referred to as "warhead", have been used in the design of some enzyme inhibitors [52, 53]. The aminopyridine group performs electronic interactions thanks to its nucleophilic character, while it can form hydrogen bond interaction with organic molecules due to its amino group. In addition, the pharmacokinetic properties of molecules containing the aminopyridine group largely depend on their lipophilicity and pK_A values [54]. Recently, Krasavin et al. reported that aminonitriles can act as true inhibitors in hCA II inhibition [55]. Fouda et al. informed that in the topoisomerase catalytic activity analysis of β-enaminonitriles, these compounds inhibit both topoisomerases I and II enzymes [56]. Herein, the enzyme inhibition effects of the (NHC)$PdBr_2$(2-aminopyridine) complexes bearing benzonitrile-substituted NHC and 2-aminopyridine ligand on the carbonic anhydrase enzymes (hCA I and hCA II) and xanthine oxidase enzyme were investigated. Also, a molecular docking study was conducted to clarify the interaction of the complexes with enzymes in this study.

Results and discussion

Synthesis

The new Pd-based complexes **1a**–**1f** which contain both 2-aminopyridine and NHC ligand mixture are illustrated in Scheme 1. All complexes were synthesized from the starting material (NHC)$PdBr_2$(pyridine) complexes [57] and 2-aminopyridine. The pyridine ligand is weakly attached to the palladium center in the starting material (NHC) $PdBr_2$(pyridine) complexes [58]. The 2-aminopyridine ligand, which has a stronger nucleophilic character than pyridine, is attached to the palladium metal center via nucleophilic addition, while the pyridine which has a weak nucleophilic character is eliminated from the palladium center.

Scheme 1

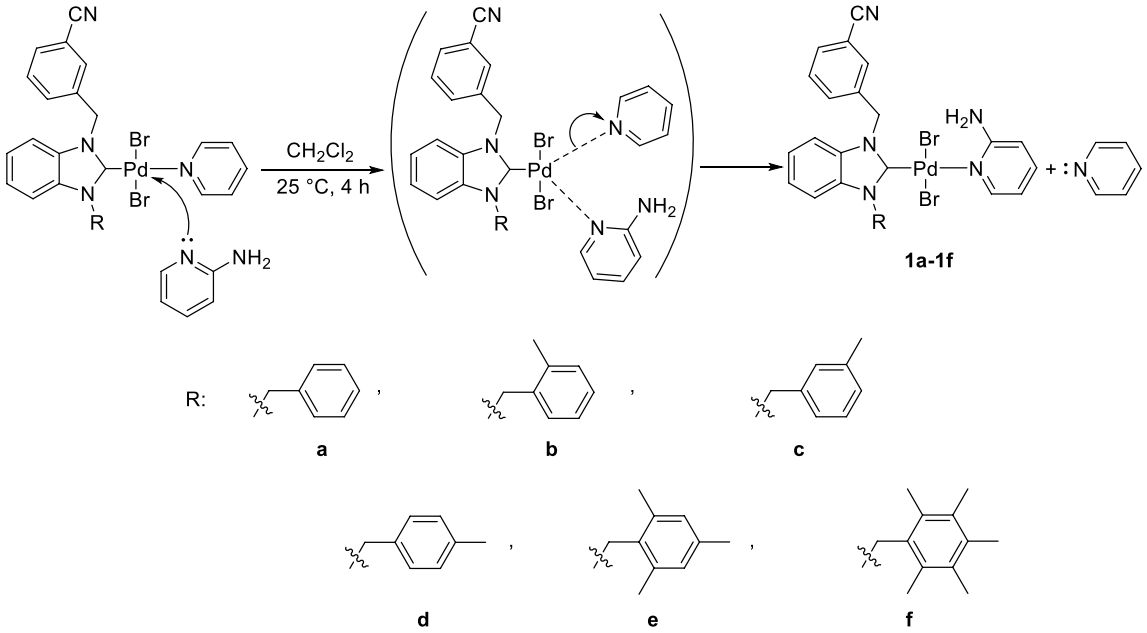

Scheme 1 .

Thus, stable (NHC)PdBr$_2$(2-aminopyridine) complexes **1a**–**1f** were synthesized as a result of the nucleophilic substitution reaction. All new (NHC)PdBr$_2$(2-aminopyridine) complexes bearing the 3-cyanobenzyl group **1a**–**1f** were obtained as a yellow solid in good yields between 76 and 82%. The formation of all complexes **1a**–**1f** was confirmed by using FT-IR, ^{1}H NMR, ^{13}C NMR spectroscopic methods, and elemental analysis. When the ^{1}H NMR spectra of the (NHC)PdBr$_2$(2-aminopyridine) complexes **1a**–**1f** were examined, the appearance of the methylene (–CH$_2$) protons for the benzyl groups next to nitrogen atoms were observed as sharp singlets in the range of 6.10 ppm and 6.39 ppm. The appearance of the amino (–NH$_2$) protons in the 2-aminopyridine between 5.30 and 6.02 ppm proved the successful synthesis. Following this, the aromatic (C–H) protons in the 2-aminopyridine groups next to nitrogen atom were observed in the range of 6.43 ppm and 6.70 ppm. The rest of the aromatic protons were observed as multiplets between 6.47 ppm and 8.08 ppm. Examination of the ^{13}C NMR spectra of the stable (NHC)PdBr$_2$(2-aminopyridine) complexes **1a**–**1f** revealed the methylene carbons (–CH$_2$) on the benzyl groups within 49.8–53.6 ppm range. The characteristic carbene (NCN) peaks for the complexes **1a**–**1f** were between 165.8 and 168.1 ppm. The characteristic nitrile (Ar–CN) carbon peaks for the complexes **1a**–**1f** were observed between 117.4 and 124.0 ppm. Following this, the aromatic carbons in the 2-aminopyridine groups next to nitrogen atom were observed between 157.1 ppm and 160.2 ppm. The rest of the aromatic carbons were in the range of 110.9–139.6 ppm. All the ^{1}H and ^{13}C NMR spectral details are given in the experimental section. The peaks at 1447, 1446, 1447, 1446, 1447, and 1444 cm^{-1} (respectively) in the FT-IR spectra verified clearly the presence of $\nu_{(\text{CN for 2-Carbene})}$ in the new complexes **1a**–**1f**. The peaks at 1628, 1626, 1627, 1626, 1626, and 1626 cm^{-1} (respectively) in the FT-IR spectra proved clearly the presence of $\nu_{(\text{CN for amino})}$ in the new complexes **1a**–**1f**. The peaks at 2323, 2231, 2228, 2231, 2228, and 2224 cm^{-1} (respectively) in the FT-IR spectrums demonstrated clearly the presence of $\nu_{(\text{CN for nitrile})}$ in the new complexes **1a**–**1f**. The peaks at 3319, 3332, 3351, 3332, 3336, and 3329 cm^{-1} (respectively) in the FT-IR spectra showed clearly the presence of $\nu_{(\text{NH})}$ in the new complexes **1a**–**1f**. All spectral data results are consistent with the literature [29].

Enzyme inhibition studies

The inhibition properties of novel (NHC)PdBr$_2$(2-aminopyridine) complexes were investigated on hCA I and hCA II by using the esterase assay method and the IC_{50} values for hCA I and hCA II are summarized in Table 1 and Fig. 1. Isoenzymes hCA I and hCA II are found in red blood cell (RBC) and needed for maintaining the physiological pH of the blood when the level of (HCO_3^-) increases [46]. In this study, the IC_{50} ranges were determined as 0.325–0.707 µM for hCA I and 0.238–0.636 µM for hCA II. In a recent study, a novel series of diamide-based benzenesulfonamides demonstrated the IC_{50} for hCAI in the range from 0.796 to 8.175 µM and for hCA II in the range from

Table 1 The inhibition values (IC_{50}) of the (NHC)$PdBr_2$(2-aminopyridine) complexes **1a**–**1f** on human carbonic anhydrase isoenzymes (hCA I and hCA II) and xanthine oxidase (XO)

Compound	XO(μM)	r^2	hCAI(μM)	r^2	hCAII(μM)	r^2
1a	1.08 ± 0.04	0.981	0.47 ± 0.03	0.994	0.54 ± 0.04	0.989
1b	0.66 ± 0.01	0.998	0.35 ± 0.05	0.977	0.46 ± 0.04	0.987
1c	1.69 ± 0.06	0.990	0.71 ± 0.04	0.988	0.64 ± 0.05	0.984
1d	0.65 ± 0.02	0.985	0.41 ± 0.03	0.989	0.34 ± 0.03	0.970
1e	0.58 ± 0.02	0.997	0.41 ± 0.04	0.997	0.24 ± 0.03	0.978
1f	0.59 ± 0.02	0.998	0.33 ± 0.02	0.993	0.32 ± 0.04	0.967
Allopurinol	2.57 ± 0.05	0.989				

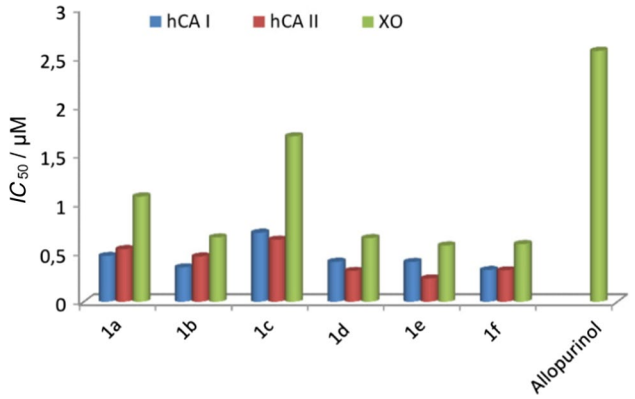

Fig. 1 The inhibition values (IC_{50}) of the (NHC)$PdBr_2$(2-aminopyridine) complexes **1a**–**1f** on human carbonic anhydrase isoenzymes (hCA I and hCA II) and xanthine oxidase enzyme (XO)

0.068 to 0.448 μM [59]. In another study, a new series of *β*-aminochalcogenides were synthesized and the IC_{50} values determined in the range from 4.6 to 22.1 μM for hCAI [60]. In addition, they newly synthesized quinazoline-linked benzensulfonamides and found the IC_{50} value range for hCAI (0.0394–3.665 μM) and hCA II (0.75–833.1 nM) [61]. Our results showed that all of the synthesized new 3-cyanobenzyl-substituted (NHC)$PdBr_2$(2-aminopyridine) complexes effectively inhibited hCA I and hCA II. Due to the high inhibitor activity of (NHC)$PdBr_2$(2-aminopyridine) complexes toward CA isoenzymes, it might be used as an interesting therapeutic which could be utilized for the treatment of a wide number of disorders such as oxidative stress, anemia, cancer, edema, osteoporosis, and obesity [38, 39].

In vitro inhibition effect of (NHC)$PdBr_2$(2-aminopyridine) complexes on serum bovine XO was also measured spectrophotometrically by following the increase in uric acid levels at 294 nm [47]. Allopurinol was included as a positive control to compare the IC_{50} values. All the NHC compounds have potential inhibition effects more than allopurinol. The IC_{50} for enzyme inhibition range that we found (0.576–1.693 μM) is summarized in Table 1 and Fig. 1. A recent study demonstrated the IC_{50} for XO (0.263–20.45 μM) for newly synthesized hesperidin derivatives [62]. In another study, a research groups synthesized coumarin derivatives, investigated the biological activity and reported that IC_{50} value range was 14.79–97.65 μM [63]. In another study, a series of *N*-(4-alkoxy-3-cyanophenyl)-isonicotinamide/nicotinamide derivatives were synthesized, evaluated for their inhibitory potency in vitro against XO and IC_{50} measured as 0.3–35.0 μM [64].

Recently, studies on the antibacterial and anticancer activities of novel synthesized benzonitrile-substituted NHC precursors and their silver complexes have attracted attention [63–66]. In these studies, benzonitrile-substituted NHC precursors and their silver complexes exhibited anticancer and antibacterial activity [65–68]. In these studies, benzonitrile-substituted NHC precursors and their silver complexes exhibited anticancer and antibacterial activity [65–68]. According to our results, it may be stated that metal–NHC complexes containing benzonitrile and 2-aminopyridine exhibited good biological activity in terms of enzyme inhibition properties. The benzonitrile functional group reacts easily with biological molecules such as amino acids in the enzyme structure thanks to its electronic properties. The aminopyridine group performs electronic interactions thanks to its nucleophilic character with organic molecules. Also, this group can form hydrogen bond interaction with organic molecules such as amino acid molecules due to its amino group in the structure. Other groups (aryl/alkyl) in our complexes are important in terms of secondary interaction such as electronic inductive effect and steric bulky in enzyme inhibition activity of the complexes. Our results are also parallel to those in literature [55].

Molecular docking studies

The new synthesized (NHC)$PdBr_2$(2-aminopyridine) complexes **1a**–**1f** were screened in vitro for their inhibition activity using different cancer targets. The xanthine oxidase enzyme (XO) and human carbonic anhydrase isoenzymes (hCA I and hCA II) were employed for these comparative studies through molecular docking using Discovery Studio 2019. The hydrophilic and hydrophobic interactions of allopurinol in binding site of XO formed noticeable important residues such as Ser876, Glu879, Arg880, Phe 914, Phe1009, Ala1078, and Ala1079. In

line with this result, the binding pattern of ligands was carefully investigated and evaluated. At the same time, the in vitro data of the related ligands are helpful to compare with their computational results.

The first attention case is that all the ligands are quite effective compared to the reference ligand against the XO target based on their in vitro data. This was easily explained with the help of molecular docking results. Based on the structure of allopurinol, which is expressed in yellow, the related ligands have a larger surface area, as seen in Fig. 2. For this reason, they have more interactions (electrostaic and hydrophobic) in the binding site of the target, especially, **1e** and **1f** complexes, which have better inhibition effects than reference ligand and others (**1a**–**1d**), show supporting results in Fig. 2 and Table S1.

The complex **1f** can be compared with active complex **1e**; the optimum number (three) and positions (ortho and para) of methyl group on phenyl ring of complex **1e** might be the dominant cause for the inhibition effect and these were absent in **1a**, **1b**, **1c**, and **1d**. The complex **1f** has more methyl groups than **1e**. But this state causes an undesired effect like less inhibition effect on XO.

Furthermore, the same process was performed to the same ligands against hCA I and hCA II. Figure 3 shows that compound **1f** has the best inhibition effect than others, because it has 19 non-bonding interactions with hCA I including three hydrogen bonds with Thr199 (2.76 Å), His200 (2.11 Å), and His 67 (2.18 Å) residues of the enzyme, and also 16 hydrophobic interactions with His94, Pro3, Pro202, Ala135, Leu198, Trp5, Tyr20,His67, and His200 residues in the binding site of hCA I. The molecular docking results obtained for hCA II are similar to those obtained with the XO target in Fig. 4.

Besides interactions of the ligands, binding energy values of the (NHC)PdBr$_2$(2-aminopyridine) complexes **1a**–**1f** on each target were calculated and analyzed as given in Table 2.

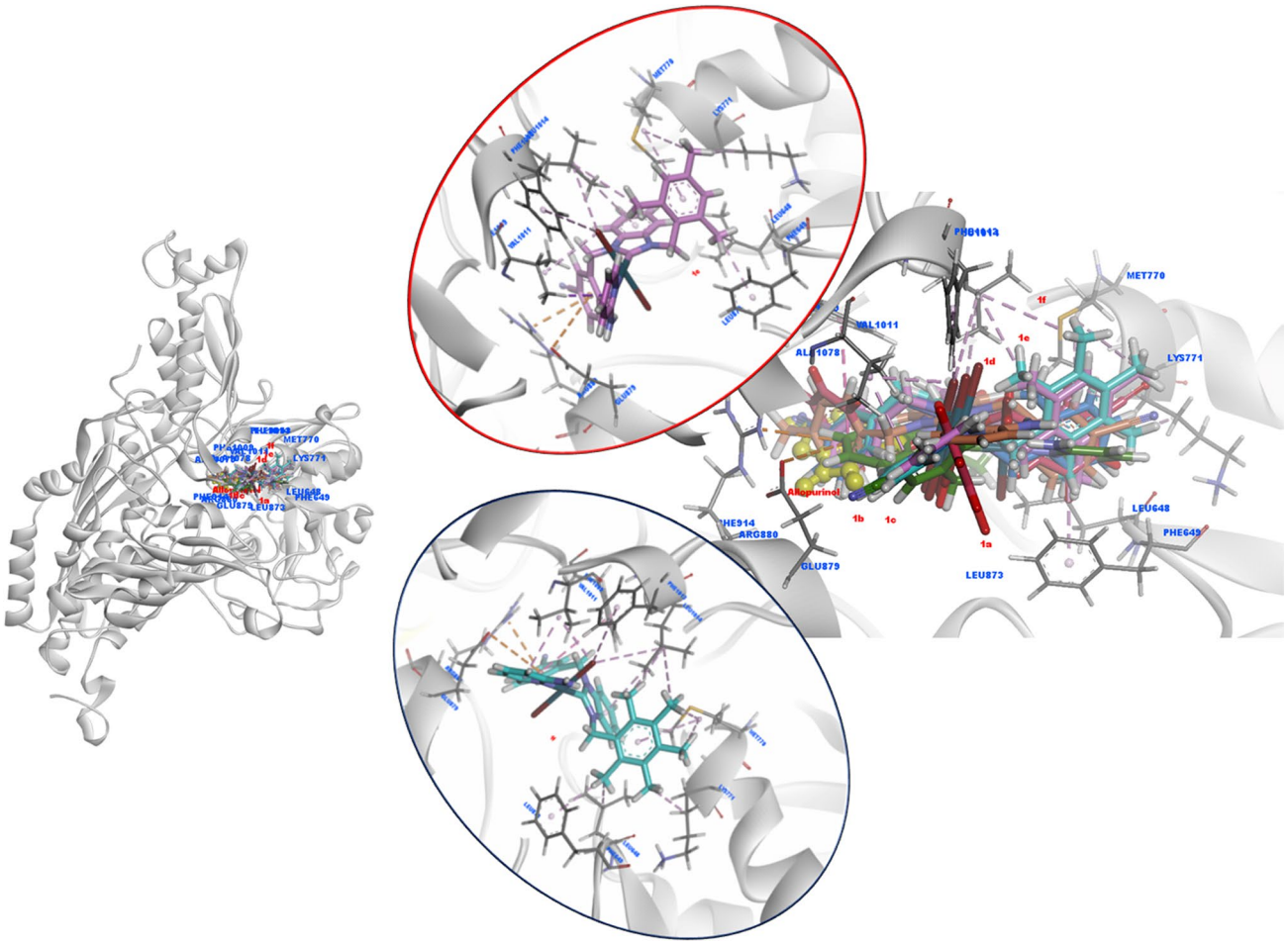

Fig. 2 Representation of 3D interaction of 3NVY with the (NHC)PdBr$_2$(2-aminopyridine) complexes **1a**–**1f** which were marked with different colors in the active site of XO (**1a** colored claret red; **1b** colored blue; **1c** colored green; **1d** colored orange; **1e** colored light pink, and **1f** colored light blue) (color figure online)

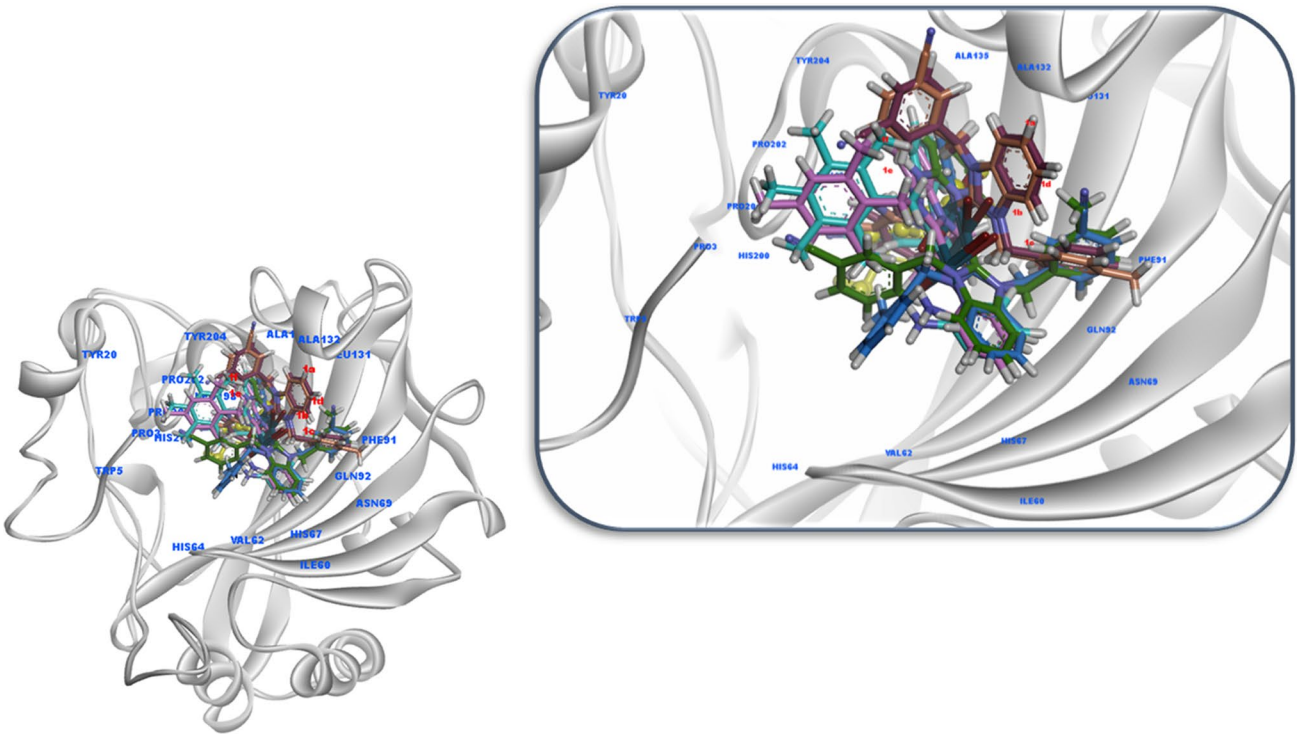

Fig. 3 Representation of 3D interaction of 1AZM with the (NHC)$PdBr_2$(2-aminopyridine) complexes **1a**–**1f** at the active site

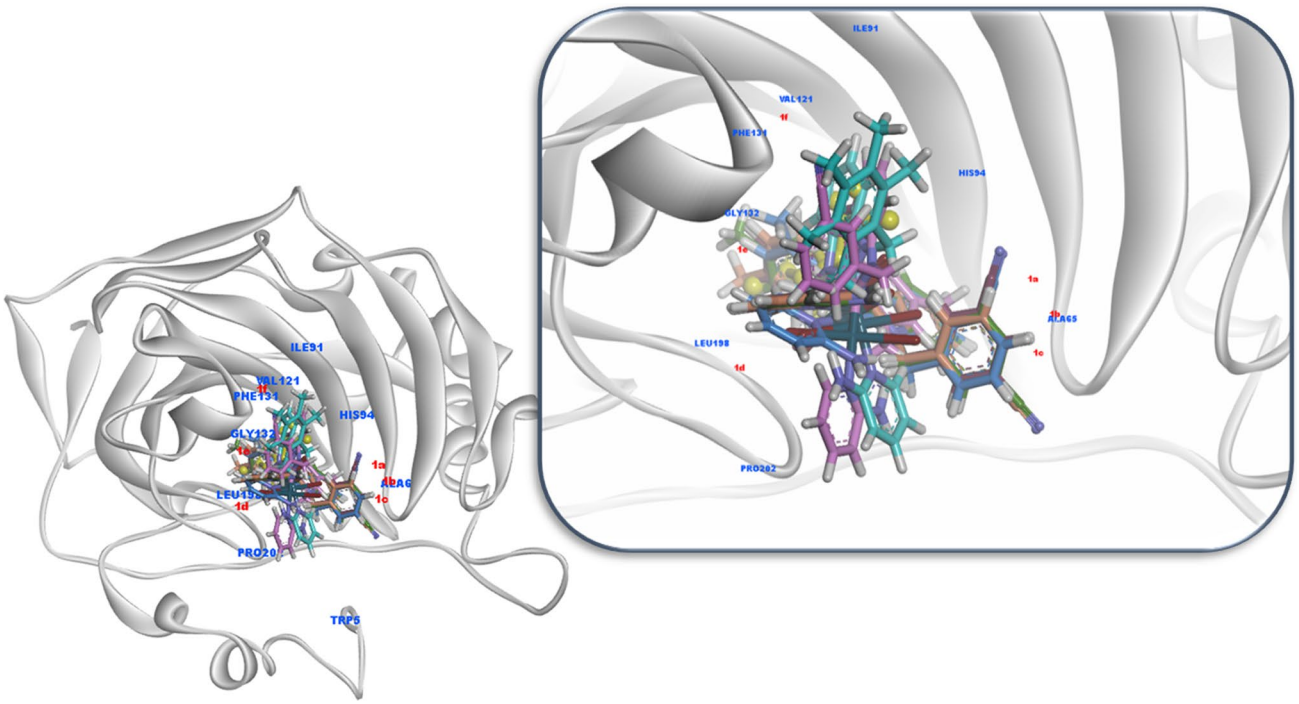

Fig. 4 Representation of 3D interaction of 3HS4 with the (NHC)$PdBr_2$(2-aminopyridine) complexes **1a**–**1f** at the active site

Further, the correlation between the binding energy values of the studied compounds and inhibition constant IC_{50} values was studied and plotted in Fig. 5, which displays a linear relationship. In the analysis of CDOCKER

Table 2 Binding energy values of the (NHC)PdBr$_2$(2-aminopyridine) complexes **1a–1f**

Binding energy/kJ mol^{-1}			
Compounds	XO	CAI	CAII
1a	−298.9468 ± 0.031	−226.9402 ± 0.031	−313.9674 ± 0.042
1b	−329.5737 ± 0.045	−214.3045 ± 0.052	−287.9010 ± 0.030
1c	−277.8176 ± 0.023	−234.9316 ± 0.036	−322.8374 ± 0.032
1d	−299.5326 ± 0.022	−263.2573 ± 0.041	−321.5822 ± 0.065
1e	−321.9588 ± 0.015	−244.4711 ± 0.065	−263.4246 ± 0.011
1f	−328.1511 ± 0.020	−255.6006 ± 0.016	−265.3493 ± 0.019

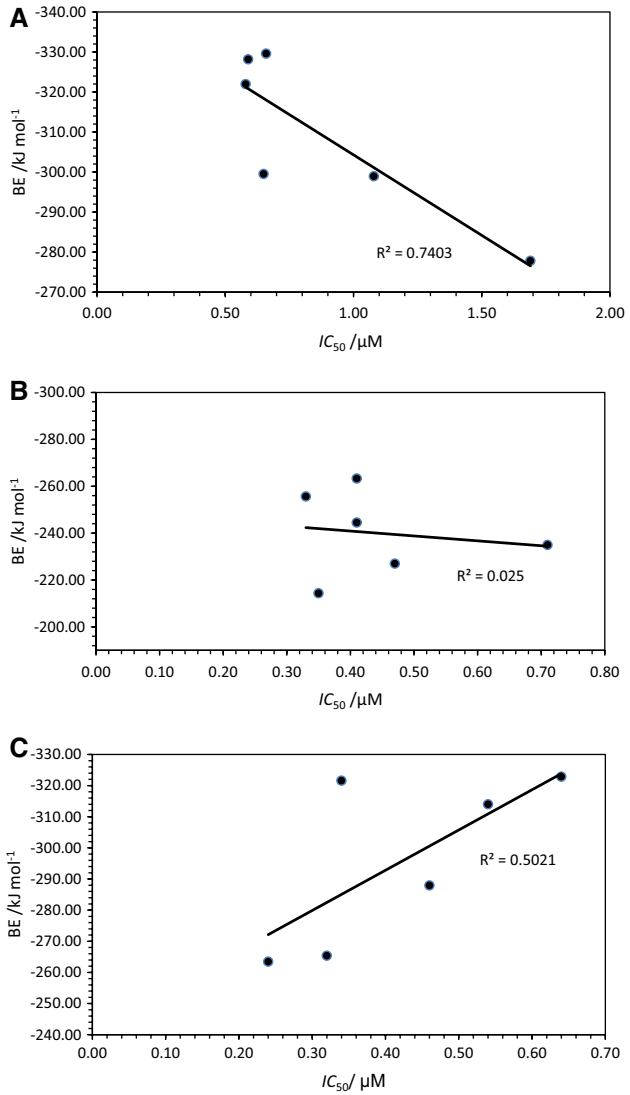

Fig. 5 The correlation between the experimental $IC_{50,}$ (µM) values and the binding energy (kJ mol) values of new-synthesized complexes toward **a** XO, **b** hCA I and **c** hCA II

docking results, a high correlation ($R^2 = 0.7403$) between IC_{50} of the studied compounds against XO and binding energy was seen as shown in Fig. 5a. In the case of hCA II, the correlation between IC_{50} and binding energy was moderate, $R^2 = 0.5021$ (Fig. 5c), whereas a poor correlation ($R^2 = 0.025$) was identified between binding energy and IC_{50} of hCA I ,as illustrated in Fig. 5b. Therefore, binding energy has the best capability to rank the bioactivities of the studied inhibitors for XO; this finding is consistent with that of Yan et al. [69], who reported that binding energy was in good correlation ($R^2 = 0.7236$) with IC_{50} of the ligands as inhibitors for COX-2. But binding energy is not the best choice for both hCA I and hCA II. The findings of this study could be promising in the future for development of effective drug for XO.

Conclusions

Consequently, this study contains the synthesis and inhibitor applications of the new 3-cyanobenzyl-substituted (NHC)PdBr$_2$(2-aminopyridine) complexes. All of the new complexes were characterized using FT-IR spectroscopy, ^{1}H NMR, ^{13}C NMR and elemental analysis techniques. The characterization data were consistent with the proposed formulas. The new (NHC)PdBr$_2$(2-aminopyridine) complexes **1a–1f** were used to determine the efficient inhibition against CA isoenzymes, and xanthine oxidase (XO) enzymes. Therefore, these complexes may be effective inhibitors of hCA and XO enzymes due to nano- and micromolar levels of IC_{50}. Also, the docking calculations exhibited favorable binding between the new (NHC)PdBr$_2$(2-aminopyridine) complexes **1a–1f** and three targets. The results of the docking studies based on the related new (NHC)PdBr$_2$(2-aminopyridine) complexes **1a–1f** with three targets, including XO and hCA I and hCA II, confirmed the experimental data. The impact of these compounds on binding sites of XO, hCA I, and hCA II was carefully investigated and interpreted according to their interactions types and binding energy value using molecular docking.

Experimental

All synthesis for the new Pd-based complexes **1a**–**1f** containing both 2-aminopyridine and NHC ligand mixture were prepared under an inert argon atmosphere by using standard Schlenk techniques. All solvents were used without any drying or purification. All reagents were economically accessible from Alfa Aesar, Sigma-Aldrich, AFG Bioscience, Merck, and Acros Organics Chemical Co., and utilized without subsequent purification. The synthesis of *meta*-cyanobenzyl-substituted Pd-PEPPSI complexes [57] used as the starting material in this study was synthesized in Inonu University Catalysis Research and Application Center Laboratory. Furthermore, melting points were recognized in glass capillaries under air with an Electrothermal-9200 melting point apparatus. On the other hand, FT-IR spectra assays were kept in the range 400–4000 cm^{-1} on Perkin Elmer Spectrum 100 FT-IR spectrometer using KBr discs. Carbon (^{13}C) and proton (^{1}H) NMR spectra were recorded using either a Bruker Avance III 400 MHz NMR spectrometer operating at 100 MHz (^{13}C), 400 MHz (^{1}H) in DMSO-d_6 and $CDCl_3$ with tetramethylsilane as an internal reference by Inonu University Catalysis Research and Application Center. Elemental analyses were performed by Inonu University Scientific and Technology Centre (Malatya, Turkey).

Dibromo[1-benzyl-3-(3-cyanobenzyl)benzimidazol-2-ylidene](2-aminopyridine)palladium(II) (1a, $C_{27}H_{23}Br_2N_5Pd$) The complex **1a** was synthesized from the reaction of 134 dibromo[1-benzyl-3-(3-cyanobenzyl) benzimidazol-2-ylidene]pyridinepalladium(II) (0.2 mmol) and 24 mg 2-aminopyridine (0.25 mmol) in 15 cm^3 chloroform at room temperature at 3 h [29]. Yield: 96 mg (79%); m.p.: 207–208 °C; IR (KBr): $\overline{\nu}=3319$ (NH), 2323 (C≡N for nitrile), 1628 (C–N for amino), 1447 (C–N for 2-$C_{carbene}$) cm^{-1}; ^{1}H NMR (400 MHz, DMSO-d_6): $\delta=8.32$ (d, 1H, $J=4.8$ Hz, –$NC_5\boldsymbol{H}_4NH_2$), 7.95–7.31 (m, 14H, Ar–***H***), 6.68 (m, 2H, –$NC_5\boldsymbol{H}_4NH_2$), 6.36 (s, 2H, –$NC\boldsymbol{H}_2C_6H_4CN$), 6.30 (s, 2H, –$NC\boldsymbol{H}_2C_6H_5$), 6.02 (s, 2H, –$NC_5H_4N\boldsymbol{H}_2$) ppm; ^{13}C NMR (100 MHz, DMSO-d_6): $\delta=168.1$ (Pd–$\boldsymbol{C}_{carbene}$), 159.3 (amino-pyr $\boldsymbol{C}_1$), 151.4 (amino-pyr $\boldsymbol{C}_5$), 139.6, 136.5, 136.3, 136.1, 135.1, 134.0, 131.3, 129.1, 128.6, 125.5 (Ar–***C***), 124.0 (***C***≡N), 112.2 (amino-pyr $\boldsymbol{C}_4$), 112.1(amino-pyr $\boldsymbol{C}_3$), 111.4 (Ar–***C***), 108.7 (amino-pyr $\boldsymbol{C}_2$), 52.2 (–N***C***H-$_2C_6H_4CN$), 51.8 (–N***C***$H_2C_6H_5$) ppm.

Dibromo[1-(3-cyanobenzyl)-3-(2-methylbenzyl)benzimidazol-2-ylidene](2-aminopyridine)palladium(II) (1b, $C_{27}H_{23}Br_2N_5Pd$) The complex **1b** was synthesized by using the same method mentioned for **1a**, using 137 mg dibromo[1-(3-cyanobenzyl)-3-(2-methylbenzyl)benzimidazol-2-ylidene]pyridinepalladium(II) (0.2 mmol). Yield: 104 mg (76%); m.p.: 228–229 °C; IR (KBr) $\overline{\nu}=3332$ (NH), 2331 (C≡N for nitrile), 1626 (C–N for amino), 1446 (C–N for 2-$C_{carbene}$) cm^{-1}; ^{1}H NMR (400 MHz, DMSO-d_6): $\delta=8.18$ (s, 1H, –$NC_5\boldsymbol{H}_4NH_2$), 8.06–7.07 (m, 13H, Ar–***H***), 6.64 (m, 2H, –$NC_5\boldsymbol{H}_4NH_2$), 6.39 (s, 2H, –$NC\boldsymbol{H}_2C_6H_4CN$), 6.25 (s, 2H, –$NC\boldsymbol{H}_2C_6H_4CH_3$), 5.90 (s, 2H, –$NC_5H_4N\boldsymbol{H}_2$), 2.59 (s, 3H, –$NCH_2C_6H_4C\boldsymbol{H}_3$) ppm; ^{13}C NMR (100 MHz, DMSO-d_6): $\delta=168.0$ (Pd–$\boldsymbol{C}_{carbene}$), 159.1 (amino-pyr $\boldsymbol{C}_1$), 149.0 (amino-pyr $\boldsymbol{C}_5$), 137.9, 134.7, 134.0, 133.9, 132.2, 130.3, 127.9, 124.1, 122.9 (Ar–***C***), 119.1 (***C***≡N), 112.8 (amino-pyr $\boldsymbol{C}_3$), 112.0 (amino-pyr $\boldsymbol{C}_4$), 111.4 (Ar–***C***), 105.3 (amino-pyr $\boldsymbol{C}_2$), 51.7 (–$NC\boldsymbol{H}_2C_6H_4CN$), 50.3 (–N***C***H-$_2C_6H_4CH_3$), 19.8 (–$NCH_2C_6H_4\boldsymbol{C}H_3$) ppm.

Dibromo[1-(3-cyanobenzyl)-3-(3-methylbenzyl)benzimidazol-2-ylidene](2-aminopyridine)palladium(II) (1c, $C_{28}H_{25}Br_2N_5Pd$) The complex **1c** was synthesized by using the same method mentioned for **1a**, using 137 mg dibromo[1-(3-cyanobenzyl)-3-(3-methylbenzyl)benzimidazol-2-ylidene]pyridine palladium(II) (0.2 mmol). Yield: 112 mg (80%); m.p.: 170–171 °C; IR (KBr) $\overline{\nu}=3351$ (NH), 2228 (C≡N for nitrile), 1627 (C–N for amino), 1447 (C–N for 2-$C_{carbene}$) cm^{-1}; ^{1}H NMR (400 MHz, $CDCl_3$): $\delta=8.27$ (s, 1H, –$NC_5\boldsymbol{H}_4NH_2$), 7.91–7.07 (m, 13H, Ar–***H***), 6.63, 6.51 (s, 2H, –$NC_5\boldsymbol{H}_4NH_2$), 6.23 (s, 2H, –$NC\boldsymbol{H}_2C_6H_4CN$), 6.16 (s, 2H, –$NC\boldsymbol{H}_2C_6H_4CH_3$), 5.34 (s, 2H, –$NC_5H_4N\boldsymbol{H}_2$), 2.35 (s, 3H, –$NCH_2C_6H_4C\boldsymbol{H}_3$) ppm; ^{13}C NMR (100 MHz, $CDCl_3$): $\delta=167.1$ (Pd–$\boldsymbol{C}_{carbene}$), 158.2 (amino-pyr $\boldsymbol{C}_1$), 152.6 (amino-pyr $\boldsymbol{C}_5$), 149.4 (amino-pyr $\boldsymbol{C}_5$), 138.7, 134.8, 134.4, 132.5, 132.1, 131.5, 129.9, 129.1, 128.8, 125.1, 123.7, 123.6 (Ar–***C***), 118.4 (***C***≡N), 114.3 (Ar–***C***), 113.0 (amino-pyr $\boldsymbol{C}_3$), 111.8 (amino-pyr $\boldsymbol{C}_4$), 111.4 (Ar–***C***), 110.8 (amino-pyr $\boldsymbol{C}_2$), 53.6 (–$NC\boldsymbol{H}_2C_6H_4CN$), 52.3 (–N***C***$H_2C_6H_4CH_3$), 21.4 (–$NCH_2C_6H_4\boldsymbol{C}H_3$) ppm.

Dibromo[1-(3-cyanobenzyl)-3-(4-methylbenzyl)benzimidazol-2-ylidene](2-aminopyridine)palladium(II) (1d, $C_{28}H_{25}Br_2N_5Pd$) The complex **1d** was synthesized by using the same method mentioned for **1a**, using 137 mg dibromo[1-(3-cyanobenzyl)-3-(4-methylbenzyl)benzimidazol-2-ylidene]pyridine palladium(II) (0.2 mmol). Yield: 109 mg (78%); m.p.: 215–216 °C; IR (KBr) $\overline{\nu}=3332$ (NH), 2231 (C≡N for nitrile), 1626 (C–N for amino), 1446 (C–N for 2-$C_{carbene}$) cm^{-1}; ^{1}H NMR (400 MHz, $CDCl_3$): $\delta=8.21$ (m, 1H, –$NC_5\boldsymbol{H}_4NH_2$), 7.84–7.05 (m, 13H, Ar–***H***), 6.56, 6.43 (d, m, 2H, $J=8.4$ Hz, –$NC_5\boldsymbol{H}_4NH_2$), 6.15 (s, 2H, –$NC\boldsymbol{H}_2C_6H_4CN$), 6.11 (s, 2H, –$NC\boldsymbol{H}_2C_6H_4CH_3$), 5.30 (s, 2H, –$NC_5H_4N\boldsymbol{H}_2$), 2.28 (s, 3H, –$NCH_2C_6H_4C\boldsymbol{H}_3$) ppm; ^{13}C NMR (100 MHz, $CDCl_3$): $\delta=165.8$ (Pd–$\boldsymbol{C}_{carbene}$), 157.1 (amino-pyr $\boldsymbol{C}_1$), 148.3 (amino-pyr $\boldsymbol{C}_5$), 137.7, 137.1, 135.6, 131.5, 131.0, 130.6, 130.4, 128.9, 128.6, 127.0, 122.6, 122.5 (Ar–***C***), 117.4 (***C***≡N), 113.3 (amino-pyr $\boldsymbol{C}_3$), 112.0 (amino-pyr $\boldsymbol{C}_3$), 110.9 (Ar–***C***), 110.4 (amino-pyr $\boldsymbol{C}_4$), 109.7

(amino-pyr $\boldsymbol{C}_2$), 52.6 (–NC$\boldsymbol{H}_2$$C_6H_4CN$), 51.3 (–N$\boldsymbol{C}$H-$_2C_6H_4CH_3$), 20.2 (–$NCH_2C_6H_4\boldsymbol{C}H_3$) ppm.

Dibromo[1-(3-cyanobenzyl)-3-(2,4,6-trimethylbenzyl)-benzimidazol-2-ylidene](2-aminopyridine)palladium(II) (1e, $C_{28}H_{25}Br_2N_5Pd$) The complex **1e** was synthesized by using the same method mentioned for **1a**, using 142 mg dibromo[1-(3-cyanobenzyl)-3-(2,4,6-trimethylbenzyl)benzimidazol-2-ylidene]pyridine palladium(II) (0.2 mmol). Yield: 114 mg (82%); m.p.: 232–231 °C; IR (KBr) $\overline{\nu}=3336$ (NH), 2228 (C≡N for nitrile), 1626 (C–N for amino), 1447 (C–N for 2-$C_{carbene}$) cm^{-1}; ^{1}H NMR (400 MHz, DMSO-d_6): $\delta=8.13$ (s, 1H, –$NC_5\boldsymbol{H}_4NH_2$), 7.99–6.89 (m, 9H, Ar–$\boldsymbol{H}$), 6.67, 6.61 (s, d, 2H, $J=8.1$ Hz, –$NC_5\boldsymbol{H}_4NH_2$), 6.48 (s, 2H, –$NCH_2C_6\boldsymbol{H}_2(CH_3)_3$), 6.38 (s, 2H, –NC$\boldsymbol{H}_2C_6H_4CN$), 6.10 (s, 2H, –NC$\boldsymbol{H}_2C_6H_2(CH_3)_3$), 5.89 (s, 2H, –$NC_5H_4N\boldsymbol{H}_2$), 2.36, 2.32 (s, 9H, –$NCH_2C_6H_2(C\boldsymbol{H}_3)_3$) ppm; ^{13}C NMR (100 MHz, DMSO-d_6): $\delta=167.2$ (Pd–$\boldsymbol{C}_{carbene}$), 159.1 (amino-pyr $\boldsymbol{C}_1$), 149.0 (amino-pyr $\boldsymbol{C}_5$), 148.2 (amino-pyr $\boldsymbol{C}_3$), 138.5, 138.1, 137.9, 135.0, 133.9, 133.3, 132.2, 130.2, 130.0, 128.7, 123.8 (Ar–$\boldsymbol{C}$), 119.1 ($\boldsymbol{C}$≡N), 112.6 (amino-pyr $\boldsymbol{C}_4$), 112.0 (amino-pyr $\boldsymbol{C}_4$), 111.5 and 111.3 (Ar–$\boldsymbol{C}$), 108.4 (amino-pyr $\boldsymbol{C}_2$), 51.8 (–NC$\boldsymbol{H}_2C_6H_4CN$), 49.8 (–N$\boldsymbol{C}H_2C_6H_2(CH_3)_3$), 21.2 ($-NCH_2C_6H_2(\boldsymbol{C}H_3)_3$) ppm.

Dibromo[1-(3-cyanobenzyl)-3-(2,3,4,5,6-pentamethylbenzyl)benzimidazol-2-ylidene](2-aminopyridine)palladium(II) (1f, $C_{30}H_{29}Br_2N_5Pd$) The complex **1f** was synthesized by using the same method mentioned for **1a**, using 148 mg dibromo[1-(3-cyanobenzyl)-3-(2,3,4,5,6-pentamethylbenzyl)benzimidazol-2-ylidene]pyridine palladium(II) (2 mmol). Yield: 115 mg (79%); m.p.: 246–247 °C; IR (KBr) $\overline{\nu}=3329$ (NH), 2224 (C≡N for nitrile), 1626 (C–N for amino), 1444 (C–N for 2-$C_{carbene}$) cm^{-1}; ^{1}H NMR (400 MHz, DMSO-d_6): $\delta=8.14$ (s, 1H, –$NC_5\boldsymbol{H}_4NH_2$), 8.08–6.47 (m, 9H, Ar–$\boldsymbol{H}$), 6.70, 6.62 (t, m, 2H, $J=5.7$ Hz, –$NC_5\boldsymbol{H}_4NH_2$), 6.38 (s, 2H, –NC$\boldsymbol{H}_2C_6H_4CN$), 6.19 (s, 2H, –NC$\boldsymbol{H}_2C_6(CH_3)_5$), 5.90 (s, 2H, –$NC_5H_4N\boldsymbol{H}_2$), 2.35, 2.27 (d, s, 15H, $J=4.3$ Hz, –$NCH_2C_6(C\boldsymbol{H}_3)_5$) ppm; ^{13}C NMR (100 MHz, DMSO-d_6): $\delta=167.0$ (Pd–$\boldsymbol{C}_{carbene}$), 160.2 (amino-pyr $\boldsymbol{C}_1$), 159.1 (amino-pyr $\boldsymbol{C}_1$), 149.0 (amino-pyr $\boldsymbol{C}_5$), 148.1 (amino-pyr $\boldsymbol{C}_5$), 138.5, 138.1, 137.9, 137.4, 135.8, 134.4, 134.0, 133.3, 133.2, 132.2, 130.2, 128.4, 123.6 (Ar–$\boldsymbol{C}$), 119.1 ($\boldsymbol{C}$≡N), 112.7 (amino-pyr $\boldsymbol{C}_3$), 112.2 (amino-pyr $\boldsymbol{C}_4$), 111.9, 111.5 (Ar–$\boldsymbol{C}$), 108.4 (amino-pyr $\boldsymbol{C}_2$), 51.8 (–NC$\boldsymbol{H}_2C_6H_4CN$), 51.4 (–N$\boldsymbol{C}H_2C_6(CH_3)_5$), 17.9, 17.5, 17.2 ($-NCH_2C_6(\boldsymbol{C}H_3)_5$) ppm.

Biochemical studies

The purification of hCA isoenzymes (hCA I and hCA II) was performed considering the methods defined previously by Göcer et al. [70]. The isoenzymes were purified via affinity column Sepharose-4B-L-tyrosine-sulfanilamide with single step. Then, the protein quantity in the purification stage was measured by Bradford method spectrophotometrically. The CA activity was assayed with the method reported by Verpoorte et al. [71]. The differences in absorbance at 348 nm of 4-nitrophenyl acetate (NPA) to 4-nitrophenylate were noted. 4-NPA was utilized as the substrate. The reaction mixture included purified enzyme, distilled water, 4-NPA (3.0 mM), and Tris–SO_4 buffer (50 mM, pH 7.4). Inhibition experiments were conducted with different concentrations of the inhibitor. Table 1 and Fig. 1 show the IC_{50} values for the NHC.

In vitro inhibition of xanthine oxidase (ox) enzyme

The XO inhibitory effect was determined spectrophotometrically by measuring the formation of uric acid. The assay mixture contained XO enzyme (0.2 U), phosphate buffer (50 mM, pH 7.4), tested NHC, and xanthine (1 mM). After the preincubation of the assay mixture at 37 °C for 10 min, the reaction was initiated by adding freshly prepared xanthine. The formation of uric acid was measured kinetically for 2 min at 294 nm. Allopurinol was utilized as a positive control. The percentage of inhibitory activity was assayed by comparing the reaction rate of the compound-treated group to that of the positive reference. Then, IC_{50} of XO inhibition was calculated as follows:

$$\text{Xanthine oxidase inhibition}\,(\%) = \left(A_{\text{control}} - A_{\text{sample}} / A_{\text{control}}\right) \times 100.$$

Molecular docking

The present molecular docking was performed to determine the binding of the new (NHC)$PdBr_2$(2-aminopyridine) complexes **1a**–**1f** in three different targets, xanthine oxidase (XO) and human carbonic anhydrases (CA) having hCA I and hCA II. The CDOCKER is a grid-based molecular docking method that employs CHARMm for molecular docking. The crystal structures of XO with allopurinol as reference ligand, hCA I and hCA II were obtained from Protein Data Bank (PDB: 3NVY, 1AZM, and 3HS4, respectively). Before starting the docking process, the 3D structures were optimized by removing water molecules, metals and ligand from crystal structures. All the (NHC)$PdBr_2$(2-aminopyridine) complexes **1a**–**1f** were sketched and minimized using density functional theory (DFT) at B3LYP/SDD level implemented in Gaussian09 [72]. Then the conformational analysis of these complexes was analyzed using CHARMm as implemented in Discovery Studio 2019 [73]. CDOCKER was employed for molecular docking study. The results of

molecular docking were evaluated depending on CDOCKER score and non-bonding interactions of each complex against the related targets.

Acknowledgements This study was financially supported by Inonu University Research Fund (Project Code: FYL-2019-1446 and FBG-2018-1569). The authors thank the Inonu University Faculty of Science Department of Chemistry for the spectroscopy and elemental analysis characterization of compounds.

References

1. Wanzlik H-W, Schönherr H-J (1968) Angew Chem Int Ed 7:141
2. Arduengo AJ, Harlow RL, Kline M (1991) J Am Chem Soc 113:361
3. Arduengo AJ, Goerlich JR, Marshall WJ (1995) J Am Chem Soc 117:11027
4. He X-X, Li Y, Ma B-B, Ke Z, Liu F-S (2016) Organometallics 38:2655
5. Crudden CM, Allen DP (2004) Coord Chem Rev 248:2247
6. Fortman GC, Nolan SP (2011) Chem Soc Rev 40:5151
7. Jana R, Pathak TP, Sigman MS (2011) Chem Rev 111:1417
8. Aktaş A, Barut Celepci D, Gök Y, Aygün M (2018) ChemistrySelect 3:10932
9. Erdemir F, Barut Celepci D, Aktaş A, Gök Y (2019) ChemistrySelect 4:5585
10. Wantz M, Bouché M, Dahm G, Chekkat N, Fournel S, Bellemin-Laponnaz S (2018) Int J Mol Sci 19:3472
11. Aktaş A, Gök Y (2014) Transit Met Chem 39:925
12. Aktaş A, Gök Y (2015) Catal Lett 145:631
13. Sarı Y, Aktaş A, Barut Celepci D, Gök Y, Aygün M (2017) Catal Lett 147:2340
14. Matharu AS, Ahmed S, Almonthery B, Macquarrie DJ, Lee Y-S, Kim Y (2018) Chemsuschem 11:716
15. Berthel JHJ, Tendera L, Kuntze-Fechner MW, Kuehn L, Radius U (2019) Eur J Inorg Chem 26:3061
16. Lubitz K, Radius U (2019) Organometallics 38:2558
17. Fliedel C, Vila-Viçosa D, Calhorda MJ, Dagorne S, Avilés T (2014) ChemCatChem 6(5):1357
18. Sousa SCA, Carrasco CJ, Pinto MF, Royo B (2019) ChemCatChem 11:3839
19. Gu W-W, Chen W-J, Yan C-G (2015) Supramol Chem 27:407
20. Yıldırım I, Aktaş A, Barut Celepci D, Kırbağ S, Kutlu T, Gök Y, Aygün M (2017) Res Chem Intermed 43:6379
21. Kuehn LA, Eichhorn F, Marder TB, Radius U (2019) J Organomet Chem 881:25
22. Zinser CM, Nahra F, Falivene L, Brill M, Cordes DB, Slawin AMZ, Cavallo L, Cazin CSJ, Nolan SP (2019) Chem Commun 55:6799
23. Aktaş A, Gök Y, Akkoç S (2013) J Coord Chem 66:2901
24. Erdoğan H, Aktaş A, Gök Y, Sarı Y (2018) Transit Met Chem 43:31
25. Gök Y, Aktaş A, Erdoğan H, Sarı Y (2018) Inorg Chim Acta 471:735
26. Gök Y, Aktaş A, Sarı Y, Erdoğan H (2019) J Iran Chem Soc 16:423
27. Erdemir F, Barut Celepci D, Aktaş A, Gök Y (2020) Chem Pap 74:99
28. Aktaş A, Barut Celepci D, Kaya R, Taslimi P, Gök Y, Aygün M, Gülçin İ (2019) Polyhedron 159:345
29. Erdemir F, Barut Celepci D, Aktaş A, Gök Y, Kaya R, Taslimi P, Demir Y, Gulçin İ (2019) Bioorg Chem 91:103134
30. Curado N, Giménez N, Miachin K, Aliaga-Lavrijsen M, Cornejo MA, Jarzecki AA, Contel M (2019) ChemMedChem 14:1086
31. Roymahapatra G, Dinda J, Mishra A, Mahapatra A, Hwang W-S, Mandal SM (2015) J Cancer Res Ther 11:105
32. Chekkat N, Dahm G, Chardon E, Wantz M, Sitz J, Decossas M, Lambert O, Frisch B, Rubbiani R, Gasser G, Guichard G, Fournel S, Bellemin-Laponnaz S (2016) Bioconjugate Chem 27:1942
33. Aktaş A, Keleştemur Ü, Gök Y, Balcıoğlu S, Ateş B, Aygün M (2017) J Iran Chem Soc 15:131
34. Onar G, Gürses C, Karataş MO, Balcıoğlu S, Akbay N, Özdemir N, Ateş B, Alıcı B (2019) J Organomet Chem 886:48
35. Hussainia SY, Haque RA, Razali MR (2019) J Organomet Chem 882:96
36. Hussaini SY, Haque RA, Fatima T, Agha MT, Majid AMSA, Razali MR (2018) J Coord Chem 71:2787
37. Gül HI, Mete E, Taslimi P, Gülçin I, Supuran CT (2017) J Enzym Inhib Med Chem 32:189
38. Gieling RG, Babur M, Mamnani L, Burrows N, Telfer BA, Carta F, Winum J-Y, Scozzafava A, Supuran CT, Williams KJ (2012) J Med Chem 55:5591
39. Arechederra RL, Waheed A, Sly WS, Supuran CT, Minteer SD (2013) Bioorg Med Chem 21:1544
40. Oztaşkın N, Çetinkaya Y, Taslimi P, Goksu S, Gülçin I (2015) Bioorg Chem 60:49
41. Bhatt A, Mahon BP, Cruzeiro VWD, Cornelio B, Laronze Cochard M, Ceruso M, Roitberg A (2017) ChemBioChem 18:213
42. Guler OO, Capasso C, Supuran CT (2016) J Enzym Inhib Med Chem 31:689
43. Al-Abbasi FA (2012) Med Sci Monit 18:208
44. Borges E, Fernandes E, Roleira F (2002) Curr Med Chem 9:195
45. Gliozzi M, Malara N, Muscoli S, Mollace V (2016) Int J Cardiol 213:23
46. Lü J-M, Yao Q, Chen C (2013) Biochem Pharmacol 86:1328
47. Springer J, Tschirner A, Hartman K, Palus S, Wirth EK, Ruis SB, Möller N, von Haehling S, Argiles JM, Köhrle J, Adams V, Anker SD, Doehner W (2012) Int J Cancer 131:2187
48. Aktaş A, Erdemir F, Celepci DB, Gök Y, Aygün M (2019) Transit Met Chem 44:229
49. Miller JS, Manson JL (2001) Acc Chem Res 34:563
50. Fleming FF, Wang Q (2003) Chem Rev 103:2035
51. Larock RC (1989) Comprehensive organic transformations: a guide to functional group preparations. VCH, New York
52. Powers JC, Asgian JL, Ekici ÖD, James KE (2002) Chem Rev 102:4639
53. Silva DG, Ribeiro JFR, De Vita D, Ciannia L, Franco CH, Lucio HF-J, Moraes CB, Rocha JR, Burtoloso ACB, Kenny PW, Leitão A, Montanari CA (2017) Bioorg Med Chem Lett 27:5031
54. Rodríguez-Rangel S, Bravin AD, Ramos-Torres KM, Brugarolas P, Sánchez-Rodríguez JE (2020) Sci Rep 10:52
55. Krasavin M, Kalinin S, Zozulya S, Griniukova A, Borysko P, Angeli A, Supuran CT (2020) J Enzym Inhib Med Chem 35:165
56. Fouda AM, Assiri MA, Mora A, Ali TE, Afifi TH, El-Agrody AM (2019) Bioorg Chem 93:103289
57. Türker F, Bereket İ, Barut Celepci D, Aktaş A, Gök Y (2020) J Mol Struct 1205:127608
58. Kumar A, Katari M, Ghosh P (2013) Polyhedron 52:524
59. Abdelrahman MA, Eldehna WM, Nocentini A, Bua S, Al-Rashood ST, Hassan GS, Bonardi A, Almehizia AA, Alkahtani HM, Alharbi A, Gratteri P, Supuran CT (2019) Int J Mol Sci 20:2484
60. Tanini D, Capperucci A, Supuran CT, Angeli A (2019) Bioorg Chem 87:516
61. El-Azab AS, Abdel-Aziz AAM, Bua S, Nocentini A, El-Gendy MA, Mohamed MA, Shawer TZ, AlSaif NA, Supuran CT (2019) Bioorg Chem 87:78
62. Malik N, Dhiman P, Khatkar A (2019) Int J Biol Macromol 135:864
63. Fais A, Era B, Asthana S, Sogos V, Medda R, Santana L, Uriarte E, Matos MJ, Delogu F, Kumar A (2018) Int J Biol Macromol 120:1286

64. Zhang T, Li S, Wang L, Sun Q, Wu Q, Zhang Y, Meng F (2017) Eur J Med Chem 141:362
65. Haziz FMU, Haque AR, Amirul AA, Shaheeda N, Razali RM (2016) Polyhedron 117:628
66. Haque AR, Haziz FMU, Al-Ashraf AA, Shaheeda N, Raz-ali RM (2016) Polyhedron 109:208
67. Haque AR, Hasanudin N, Iqbal AM, Ahmad A, Hashim S, Majid AA, Ahamed KBM (2013) J Coord Chem 66:3211
68. Haque AR, Budagumpi S, Zulikha ZH, Hasanudin N, Ahamed KBM, Majid AMSA (2014) Inorg Chem Commun 44:128
69. Yan X-Q, Wang Z-C, Zhang B, Qi P-F, Li G-G, Zhu H-L (2019) Molecules 24:1685
70. Göçer H, Akıncıoglu A, Goksu S, Gulcin I (2017) Arabian J Chem 10:398
71. Verpoorte JA, Mehta S, Edsall JT (1967) J Biol Chem 242:4221
72. Frisch MJ, Trucks GW, Schlegel HB, Scuseria GE, Robb MA, Cheeseman JR, Scalmani G, Barone V, Mennucci B, Petersson GA, Nakatsuji H, Caricato M, Li X, Hratchian HP, Izmaylov AF, Bloino J, Zheng G, Sonnenberg JL, Hada M, Ehara M, Toyota K, Fukuda R, Hasegawa J, Ishida M, Nakajima T, Honda Y, Kitao O, Nakai H, Vreven T, Montgomery JA, Orti JR, Peralta JE, Ogliaro F, Bearpark M, Heyd JJ, Brothers E, Kudin KN, Staroverov VN, Kobayashi R, Normand J, Raghavachari K, Rendell A, Burant JC, Iyengar SS, Tomasi J, Cossi M, Rega N, Millam JM, Klene M, Knox JE, Cross JB, Bakken V, Adamo C, Jaramillo J, Gomperts R, Stratmann RE, Yazyev O, Austin AJ, Cammi R, Pomelli C, Ochterski JW, Martin RL, Morokuma K, Zakrzewski VG, Voth GA, Salvador P, Dannenberg JJ, Dapprich S, Daniels AD, Farkas Ö, Foresman JB (2009) Gaussian 09, Revision E.01. Gaussian Inc, Wallingford, CT, USA
73. Dassault Systemes BIOVIA (2019) Discovery studio. Dassault Systems, San Diego, CA, USA

Affiliations

Ferhat Türker[1] · Samir Abbas Ali Noma[1] · Aydın Aktaş[1,2] · Khattab Al-Khafaji[3] · Tugba Taşkın Tok[3,4] · Burhan Ateş[1] · Yetkin Gök[1]

[1] Department of Chemistry, Faculty of Arts and Sciences, Inönü University, 44280 Malatya, Turkey

[2] Vocational School of Health Service, Inonu University, 44280 Malatya, Turkey

[3] Department of Chemistry, Faculty of Arts and Sciences, Gaziantep University, 27310 Gaziantep, Turkey

[4] Department of Bioinformatic and Computational Biology, Institute of Health Science, Gaziantep University, 27310 Gaziantep, Turkey